Reduced Model For 2D Tumor Growth and Tumor Induced Angiogenesis

Mazen Alamir[1] and Mirko Fiacchini[1] and Angélique Stéphanou[2]

Abstract— **In this paper, a reduced dimensional dynamic model is proposed for drug-free tumor growth and tumor-induced angiogenesis in 2D tissues. The model involves only a few number of easily identifiable parameters and nicely captures the impact of the initial 2D vascular architecture on the future evolution of both tumor and tumor induced capillary network. The model is identified and validated using recently developed detailed model. The results remarkably fit the detailed model while being several order of magnitudes faster to simulate.**

Index Terms— **Tumor Growth, Tumor-Induced Angiogenesis, Reduced Dimensional Dynamic Model.**

I. Introduction

Modeling the dynamics underlying the tumor growth and the related mechanisms such as the tumor induced angiogenesis is a key step towards rationale optimization of cancer therapy. This is especially true when combined therapies are involved as trade-offs emerge from coupled effects each drug induces on the mechanisms being involved.

The quality of a dynamic model depends on the purpose for which it is derived. Indeed, some models are derived in order to get deeper understanding of the physiological phenomena that take place under given circumstances: these are **knowledge-based models**. These models are generally bottom-up in that they are based on detailed description of each of the mechanisms being presumably involved and the model is obtained by concatenating these elementary models. The capacity of the knowledge-based model to reproduce the experimental data is then used to validate or invalidate the assumptions that lie behind the elementary models and guide the iterative process of understanding the real-life mechanisms.

On the other hand, when the model derivation is motivated by the pragmatic goal of optimizing the therapy based on a reliable prediction of the system evolution for a family of candidate dosages, then **mechanistic models** can be more appropriate. These models (when successfully derived) can guarantee faithful prediction by matching experimental data through relationships that are not necessarily physiologically assessed. In the control system community, these are called identified models. These models can be totally data-driven (Black-Box models) or they can be based on a semi-physiological models with small number of parameters (Grey-Box models).

[1] GIPSA-lab, Grenoble Campus, 11 rue des Mathématiques, BP 46, 38402 Saint Martin d'Hères Cedex, France {mazen.alamir,mirko.fiacchini}@gipsa-lab.fr

[2]TIMC, UJF, Domaine de la Merci, 38706 La Tronche Cedex. Angelique.Stephanou@imag.fr.

Grey-Box models have been extensively used in the applied-mathematical communities to analyze optimal cancer drug delivery [11], [4], [7], [3], [6] or to design feedback laws [2], [1]. These models are generally zero-dimensional (no geometric consideration) and based on global population models. Therefore, they cannot explicitly accommodate for a specific 2D vascular architecture.

The work proposed in this paper is a part of a joint work involving several French research teams within an INSERM[1] funded project which aims at conducting experiments-based modeling effort of the 2D tumor growth and tumor induced angiogenesis in the presence of combined chemotherapy and anti-angiogenesis drugs. Experiments will be conducted on an artificially injected tumor in several rats ears and periodical measurements (2D images) will be extracted with and without drugs in order to support the modeling/identification efforts. To this respect, it seemed interesting to develop a reduced, faithful and computationally efficient grey-box model that is adapted to 2D framework and that is capable of explicit handling of the effect of specific 2D vascular architecture on the future evolution of the tumor and its vascular recruitment process.

A typical step in such modeling process is to start by modeling the drug-free case before introducing the drug effects. This is the aim of the present work. The advantages of this two-step modeling process is twofold:

1) The set of parameters are split into two separate sets so that those involved in the drug-free dynamics can be identified first.
2) The modeling of the drug-free case can inspire the way the drug effect is accounted for in the complete model. For instance, the parameters involved in the vessels recruitment by the solid tumor can be affected by the anti-angiogenesis drug injection so that non trivial coupled representation of the drug effect can be derived (rather than through simple additional and non coupled terms as it is the case in the majority of existing models). This feature is further discussed in the sequel.

The data used in the present work are those delivered by the detailed knowledge-based simulator developed in a series of papers [9], [10], [8]. This simulator has already been validated through comparison with experimental data.

This paper is organized as follows: First of all the available data are described in section II. Then section III progressively

[1]Institut National de la Santé et de la Recherche Médicale (French National Institute for Health and Medical Science)

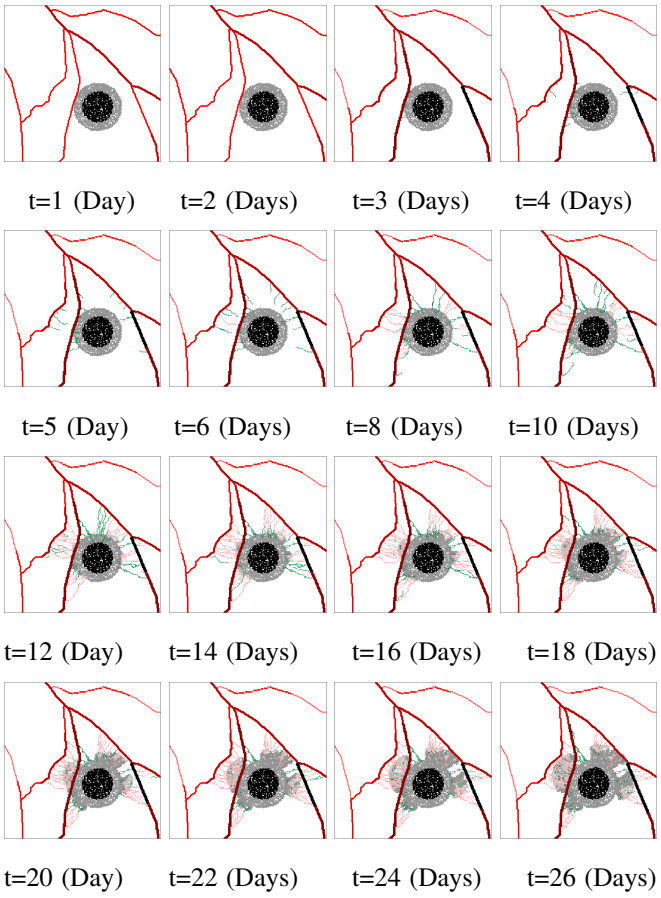

Fig. 1. Available images representing tumor and vascular network growth after solid tumor injection.

introduces the proposed model. The identification algorithm is presented in section IV. Finally, the identified model is validated in section V through simulations using different instantiations of model's dimension others than those used in the identification step. Finally, a discussion regarding the extension of the model to the case where drug is injected is proposed in section VI. The paper ends by section VII that summarizes the contributions and gives road map for future investigations.

II. Available Data

Figure 1 shows the images that are used in the present paper to derive the reduced order model for tumor and vascular network growth. The data represented in these images are produced using the detailed knowledge-based dynamic model that has been proposed and validated in [9], [10], [8]. The images show the vascular network in red and green pixels while the tumor-related pixels are given in black and gray pixels. The images show the evolution of the network during the 28 days following the injection of solid tumor.

III. Model Derivation

The derivation of the model is based on a 2D polar-coordinate partitioning of the space surrounding the solid

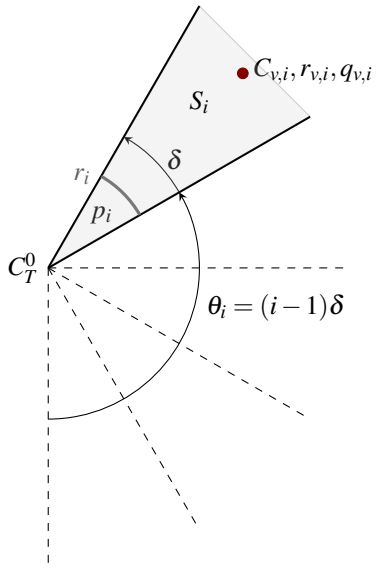

Fig. 2. Decomposition of the plane around the solid tumor into angular sectors S_i, $i \in \{1,\dots,N_s\}$

tumor as shown in the Figure 2. More precisely, the surface surrounding the tumor is decomposed into N_s angular sectors of angle δ which are all centered at the initial center of mass of the tumor denoted hereafter by C_T^0. For each of the resulting sectors S_i, $i \in \{1,\dots,N_s\}$ (defined by the angle $\theta_i = (i-1)\delta$ of the right boundary), the following quantities can be defined:

- p_i is the total number of pixels that represent the tumor cells in the sector S_i. According to the model, this can gather all black or gray-like pixels shown in Figure 1.
- $r_i(p_i)$ is the radius of the tumor in the sector S_i. This radius is directly linked to p_i according to:

$$r_i(p_i) := \sqrt{\frac{2p_i}{\delta}} \tag{1}$$

  as this radius is the one that corresponds to an angular sector of surface p_i.
- The center of mass of the parent vessels-related pixels that belong to S_i, denoted by $C_{v,i}$ and the related radius $r_{v,i}$ which is defined by $r_{v,i} := \|C_T^0 - C_{v,i}\|$. Note that one of the aims of the model is to capture the dynamics of the formation of capillary network in response to chemical stimuli released by the the solid tumor.
- The number of parent vessels related pixels $q_{v,i}$

Another key variable that does not appear in the Figure above is the amount q_i of vessels in S_i that are in direct contact with the solid tumor and which are therefore responsible of its growth. These vessels are recruited by the solid tumor provided that a neighboring parent vessel is present ($q_{v,i} \neq 0$). A geometric simple dynamic model of this recruitment process is described in the following section.

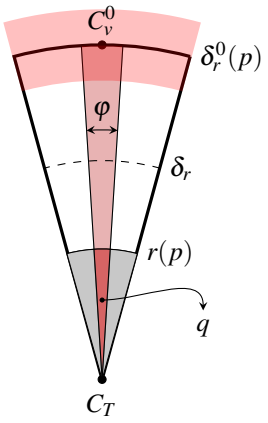

Fig. 3. Notation used in the geometric representation of the recruitment process attracting the vascular network towards the solid tumor. Note that for simplicity the index i related to the current sector is ommited.

A. A Model For Tumor Induced Angiogenesis

B. Notation and preliminary computation

Let us first of all omit the reference to the sector's number i when mentioning the above defined variables $p_i, q_i, \ldots$, etc. by simply using the notation p, q and so on keeping in mind that the model is related to a given sector S_i and that the total model will be obtained by the concatenation of all the sectors-related sub-models.

Figure 3 describes the schematic modeling of the vessels recruitment process from the parent vessels towards the solid tumor. More precisely, the amount of deviated vasculature is defined by the φ-angular sector. This amount of recruited vessels from the parent vessel is given by:

$$q_{rec} = \frac{1}{2}\left[\delta_r^0\right]^2 \times \varphi \tag{2}$$

On the other hand, in this representation, the amounts of vessels that are in contact with the solid tumor are the subset of this φ-sector that lies inside the tumor radius r. Therefore:

$$q := \frac{1}{2}\left[r(p)\right]^2 \times \varphi \tag{3}$$

Now combining (2) and (3) gives:

$$q_{rec} = \frac{1}{2}\left[\frac{\delta_r^0}{r(p)}\right]^2 \times q \tag{4}$$

Having this in mind, it is possible to compute the new distance between the solid tumor and the center of mass of the vascular network according to:

$$\delta_r \quad = \quad \frac{(q_v^0 - q_{rec}) \times \delta_r^0 + q_{rec} \times \frac{2}{3}\delta_r^0}{q_v^0}$$

which gives after straightforward manipulations:

$$\delta_r = \left[1 - \frac{1}{3}\frac{q_{rec}}{q_v^0}\right] \times \delta_r^0 \tag{5}$$

and finally, replacing q_{rec} in the last equation by its expression given by (4) gives:

$$q := 6\left[1 - \frac{\delta_r}{\delta_r^0}\right]\left[\frac{r(p)}{\delta_r^0}\right]^2 \times q_v^0 \tag{6}$$

Note that this equation links the size of the vessels that are *on the tumor*, namely q to the new distance δ_r. This relation involves both the initial topology of the vascular network (through δ_r^0 and q_v^0) and the current size of the solid tumor itself, namely $r(p)$.

Now using the notation:

$$\mathscr{T}_0 := (q_r^0, \delta_r^0) \tag{7}$$

to denote the parameters that defines the initial topology of the vascular network around the tumor and recalling that $r(p)$ depends only on p through (1), it is possible to rewrite (6) in a more compact form as follows:

$$q = Q(p, \delta_r, \mathscr{T}_0) \tag{8}$$

Note that by definition, q represents the vessels that are responsible for the tumor growth. This is precisely the quantity that is typically used in the 0-dimensional models (see for instance [5], [6]). Note however that these models involve the ratio p/q which is incompatible with the situation under study here in which initial values $q = 0$ have to be accommodated prior to the tumor induced angiogenesis and the development of the recruited capillary network.

C. Dynamic Model For Tumor Growth

In the present contribution, the growth of the tumor is defined by the following dynamic:

$$\dot{p} = p\left[\lambda_1 - \lambda_2 \ln(\frac{1+p}{1+\alpha q})\right] \quad ; \quad \lambda_1, \lambda_2 > 0 \tag{9}$$

which simply implements the following rules:

1) Growth needs pre-existing solid tumor.
2) If there is no feeding vessels ($q = 0$), the tumor stabilizes at $p_\infty := e^{\lambda_1/\lambda_2} - 1$. For the identified values of (λ_1, λ_2) (see later), p_∞ is as small as 400 which represents a tumor reduction of 70%.
3) As soon as the amount of feeding vessels q becomes sufficiently high (for the tumor size p) so as to satisfy:

$$q > q_{min}(p) := \frac{1}{\alpha}\left[\frac{1+p}{e^{\lambda_1/\lambda_2}} - 1\right] \tag{10}$$

then the tumor grows thanks to the induced angiogenesis.

Consequently, the growth model involves the three parameters $(\lambda_1, \lambda_2, \alpha)$ that need to be identified as explained later on. Now that we have the dynamic model for the tumor size p, we need to define the dynamic model that describes the evolution of the vascular network q close to the tumor. This is the aim of the next section.

D. Dynamic Model For Tumor-Induced Angiogenesis

Let us first of all notice that equation (8) suggests that either q or δ_r can be chosen (together with p) to define the state of the system for the corresponding sector since they are statically linked through (8) for a given tumor size and given vascular architecture defined through $\mathscr{T}_0$. Here, the variable δ_r is chosen for the simple reason that we dispose of direct

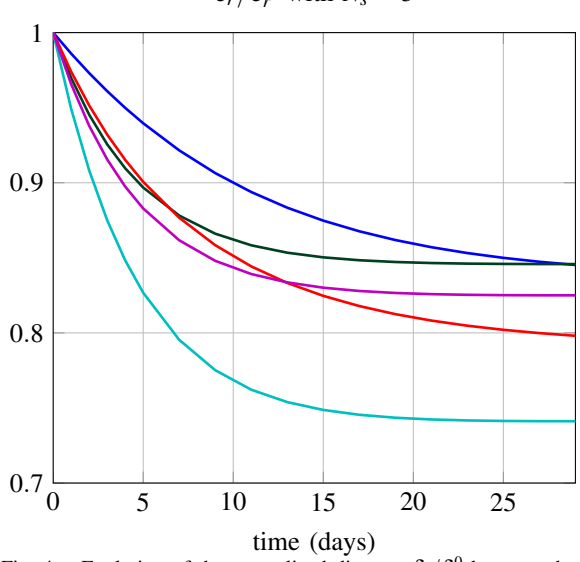

Fig. 4. Evolution of the normalized distance δ_r/δ_r^0 between the vascular network and the center of the tumor. The decrease reflects the tumor induced angiogenesis.

identification data that enables to capture the parameters of any candidate dynamic model while the very definition of q renders this difficult.

The *filtered* measured evolution of the ratio δ_r/δ_r^0 during the first 28 days following the injection of the tumor is given in Figure 4 (case of $N_s = 5$ sectors). Note that δ_r decreases because the tumor-induced angiogenesis steers the center of mass of the vascular network towards the center of the tumor (recall that δ_r designates the distance of this center of mass to the initial center of the tumor C_T^0).

Observing these plots suggests the following dynamic model for the variable δ_r:

$$\dot{\delta}_r = \frac{\lambda_r \cdot p}{\delta_r}\left[\gamma_r \delta_r^0 - \delta_r\right] \tag{11}$$

in which the two parameters $(\lambda_r, \gamma_r) \in \mathbb{R}_+ \times [0,1]$ are to be identified.

Indeed, the dynamic model (11) satisfies the following properties:

1) It shows a first order-like dynamics in accordance with the measurement.
2) It shows a *saturation*-like behavior suggesting that there is a physiological limit in vascular network migration even if the tumor continues its growth.
3) The migration takes place only if $p \neq 0$ (tumor-induced angiogenesis)
4) The higher p is, the faster is the migration process.
5) The recruitment is slower when the parent vessel is far from the tumor (presence of δ_r in the denominator of (11)).

E. The Complete Model

By gathering the tumor growth model (9) and the tumor-induced angiogenesis model (11) together with the static relation (8), one obtains the full model that is summarized as follows:

$$\begin{aligned} \dot{p} &= p\left[\lambda_1 - \lambda_2 \ln\left(\frac{1+p}{1+\alpha q}\right)\right] && (12)\\ \dot{\delta}_r &= \frac{\lambda_r \cdot p}{\delta_r}\left[\gamma_r \delta_r^0 - \delta_r\right] && (13)\\ q &= Q(p, \delta_r, \mathscr{T}_0) && (14) \end{aligned}$$

which involves five parameters $\lambda_1, \lambda_2, \alpha, \lambda_r$ and γ_r.

Before identifying these parameters, a last modification of the model is needed in order to accommodate for the necessary delay between the beginning of the vascular recruitment process and the time by which the vascular network reaches the solid tumor itself. This feature is not present in the current model (12)-(14) since according to the first order nature of (13), the distance δ_r begins immediately to decrease and this, by virtue of (14) enhances instantaneous creation of vessels at the tumor level. In order to correct this obvious inconsistency, the static relation (14) between q and δ_r is made dynamic by introducing a series of n_q filters such that one has:

$$\begin{aligned} \dot{q}_1 &= \frac{1}{\tau}\left[Q(p, \delta, \mathscr{T}_0) - q_1\right]\\ \dot{q}_2 &= \frac{1}{\tau}\left[q_1 - q_2\right]\\ &\vdots\\ \dot{q}_{n_q-1} &= \frac{1}{\tau}\left[q_{n_q-2} - q_{n_q-1}\right]\\ \dot{q} &= \frac{1}{\tau}\left[q_{n_q-1} - q\right] \end{aligned}$$

or equivalently using the transfer function notation

$$q = \left[\frac{1}{(1+\tau s)^{n_q}}\right] \cdot Q(p, \delta_r, \mathscr{T}_0) \tag{15}$$

This can also be written by using the state space representation with the following notation:

$$A(\tau) := \frac{1}{\tau}\begin{bmatrix} -1 & 0 & \dots & 0 & 0\\ +1 & -1 & \dots & 0 & 0\\ \vdots & \vdots & \dots & \vdots & \vdots\\ 0 & 0 & \dots & +1 & -1 \end{bmatrix},\ B(\tau) := \frac{1}{\tau}\begin{bmatrix} 1\\ 0\\ \vdots\\ 0 \end{bmatrix}$$
$$z := (q_1, \dots, q_{n_q-1}, q)^T,$$

the equation (15) becomes:

$$\begin{aligned} \dot{z} &= A(\tau)z + [B(\tau)]\, Q(p, \delta_r, \mathscr{T}_0) \quad ; \quad z \in \mathbb{R}^{n_q} && (16)\\ q &= (0, \dots, 0, 1)z && (17) \end{aligned}$$

Note that the filters characteristic time τ is an additional parameter of the model that has to be identified.

The final model is therefore obtained by replacing (13)-(14) by (16)-(17) and by re-introducing the reference to the

angular sector indices i for all $i \in \{1,\dots,N_s\}$, namely:

$$\dot{p}_i = p_i\left[\lambda_1 - \lambda_2 \ln(\frac{1+p_i}{1+\alpha q_i})\right] \quad (18)$$

$$\dot{\delta}_{r_i} = \frac{\lambda_r \cdot p_i}{\delta_{r_i}}\left[\gamma_r \delta_r^0 - \delta_{r_i}\right] \quad (19)$$

$$\dot{z}_i = A(\tau)z_i + [B(\tau)]\cdot Q(p_i, \delta_{r_i}, \mathscr{T}_0) \quad (20)$$

$$q_i = (0,\dots,0,1)z_i \quad (21)$$

which is a dynamic model with $n = (n_q+2)\times N_s$ states and 6 parameters to be identified that are $\lambda_1, \lambda_2, \alpha, \lambda_r, \gamma_r$ and τ. Note that the number of filters n_q is chosen in an outer loop ($n_q = 5$ seems to be appropriate).

IV. Identification Algorithm

Denoting by p the vector of parameter to be identified:

$$p := (\lambda_1, \lambda_2, \alpha, \lambda_r, \gamma_r, \tau)^T \in \mathbb{R}^6 \quad (22)$$

and the admissible set by $\mathbb{P}$:

$$\mathbb{P} := \mathbb{R}_+^4 \times [0,1] \times \mathbb{R}_+ \quad (23)$$

and given that for any choice of the number of sectors N_s, measurement is available for the tumor size p_i and the distances δ_{r_i} for $i = 1,\dots,N_s$ by processing accordingly the 2D series of images we dispose of, the optimal value p^{opt} of the parameter vector can be obtained by solving the following constrained optimization problem:

$$p^{opt} := \arg\min_{p\in\mathbb{P}} \left(\sum_{i=1}^{N_s}\sum_{k=1}^{n_t} \beta_1 \cdot \left| p_i^{pred}(t_k,p) - p_i(t_k)) \right|^2 + \beta_2 \cdot \left| \delta_{r_i}^{pred}(t_k,p) - \delta_{r_i}(t_k) \right|^2 \right) \quad (24)$$

where

- $p_i^{pred}(t_k,p)$ and $\delta_{r_i}^{pred}(t_k,p)$ are the predicted values of p_i and δ_{r_i} at instant t_k for a given value of the parameter vector p.
- β_1 and β_2 are normalizing coefficients [typically $\beta_1 = 1/\max_{i,k} p_i^2(t_k)$ and $\beta_1 = 1/\max_{i,k} \delta_{r_i}^2(t_k)$]

Note however that as in any Non Linear Programming (NLP) optimization problems, the solution can be obtained through iterative processing in which the quality of the initial guess (denoting here by p^*) is crucial in the success of the optimization task. Fortunately, the structure of the problem enables good initialization p^* of the parameter vector p to be computed as shown in Figure 5. This algorithm suggests the following comments:

- Note first that regarding the validation protocol, the parameter vector p is identified using $N_s = 18$ sectors and then the resulting optimal value p^{opt} is used to construct the models for $N_s = 9$, 18 and 36 in order to assess the robustness of the identified value on different choices of the model dimension.
- Regarding the computation of the initial guess p^*, note that the time profiles of p_i and δ_{r_i} are first filtered so that they can be derived and the derivative can be used in the definition of two separated least squares problems:

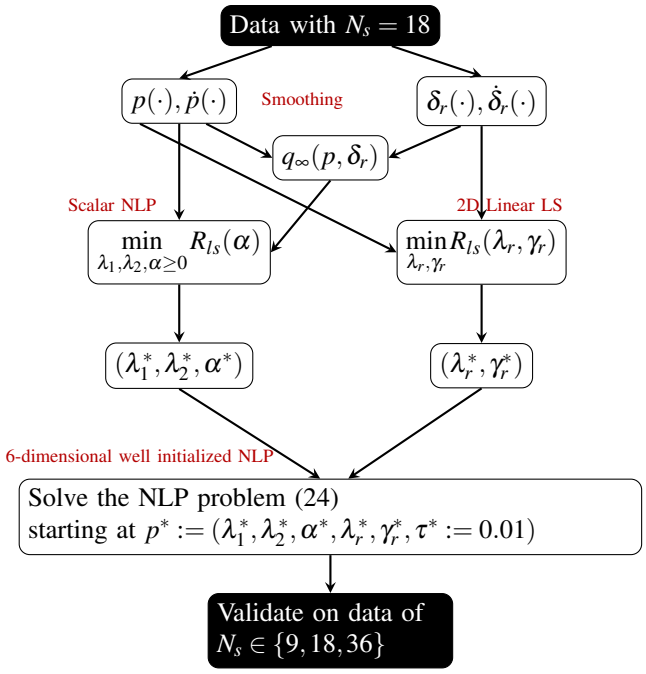

Fig. 5. The identification and the validation protocol.

1) The first is based on equation (18) in which $Q(p_i, \delta_{r_i}, \mathscr{T}_0)$ is used instead of q_i. The resulting least squares problem is solved in the unknowns $(\lambda_1, \lambda_2, \alpha)$ in a nested way (for each α, λ_1 and λ_2 are computed by solving the resulting linear least squares leading to the residual $R_{ls}(\alpha)$). This yields a scalar NLP in the variable α and the cost function $R_{ls}(\alpha)$.
2) The second is a linear least squares problem in the variables $(\lambda_r, \lambda_r\cdot\gamma_r)$ that can be formulated based on (19) and can therefore be easily solved.

- Finally, the initial value of $\alpha^* = 0.01$, it leads to almost no filtering between q_i and $Q(p_i, \delta_{r_i}, \mathscr{T}_0)$.
- The well initialized NLP problem (24) is then solved using the Matlab general purpose solver *fmincon*.

The resulting optimal set of parameters is given by:

$$\lambda_1 = 0.12,\ \lambda_2 = 0.02,\ \alpha = 0.64,\ \lambda_r = 0.009,$$
$$\gamma_r = 0.78\ ,\ \tau = 1.86\ ,\ n_q = 5$$

V. Model Validation

While the above set of parameters has been identified using the case $N_s = 18$, in the following section, the identified model is validated using three different values $N_s \in \{9, 18, 36\}$. For each of these values, the quality of the model is shown by comparing the data provided by the detailed simulation model developed in [9], [10], [8] and the data provided by the reduced model for the specified value of N_s:

1) The temporal evolution of the total tumor size: $p(t) = \sum_{i=1}^{N_s} p_i(t)$
2) The final form of the tumor in the 2D plane which is

$N_s = 9$	$N_s = 18$	$N_s = 36$
3.6%	-0.15%	2%

TABLE I
ERREUR (%) ON THE TOTAL TUMOR SIZE

$N_s = 9$	$N_s = 18$	$N_s = 36$
50 ms	70 ms	120 ms

TABLE II
COMPUTATION TIME FOR 30 DAYS SCENARIO ON A (MATLAB/MACPOWERBOOK / 2.3GHZ INTEL CORE I7)

described by the points:

$$\left(\theta_i + \frac{\delta}{2}, r(p_i)\right)_{i=1}^{N_s} \tag{25}$$

Figure 6 shows the comparison between the time profile of the total tumor during the experiments. Recall that the model parameters have been identified using the case $N_s = 18$. In that sense, the situation where $N_s = 9$ and $N_s = 36$ enable to check the extrapolation power of the model and its robustness.

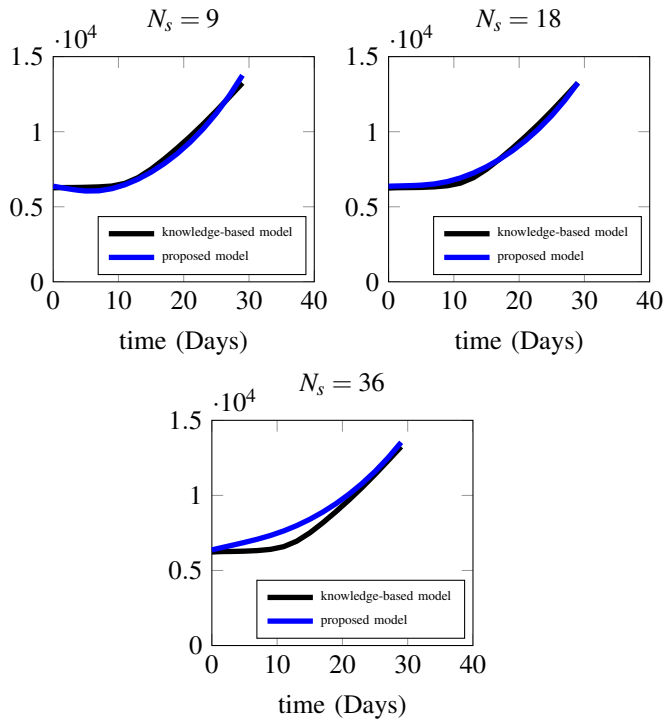

Fig. 6. Model validation: Comparison between the total tumor size prediction by the proposed model (blue) and the simulation data provided by the detailed knowledge based simulator (black). Note that the model parameters have been identified using the case $N_s = 18$.

Table I shows the erreur (in %) on the total tumor size for the different values of N_s.

Figure 7 shows the comparison between the final tumor 2D disposition as predicted by the proposed model and by the knowledge-based model. Note how the lower side of the tumor does not develop due to the absence of vascular network.

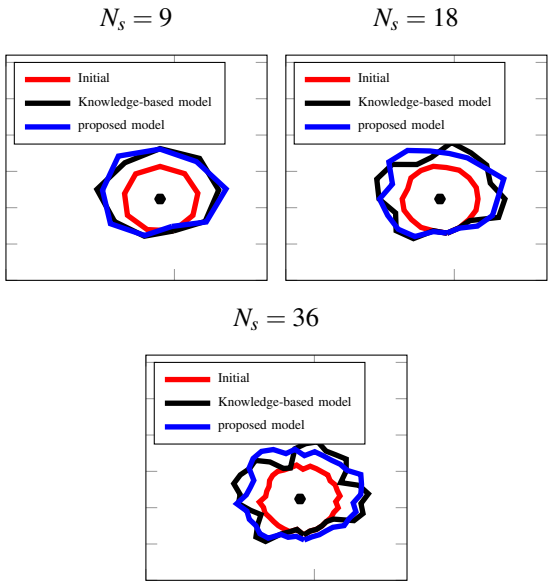

Fig. 7. Model validation: Comparison between the final 2D tumor by the proposed model (blue) and the simulation data provided by the detailed knowledge based simulator (black). The red line represents the initial disposition of the tumor. Note that the model parameters have been identified using the case $N_s = 18$.

Finally, the computation times needed to simulate the reduced model proposed in this work during the 28 days of the scenario is given in Table II. Note that the fact that the simulation can be done as fast is a crucial issue if the model should be used for a cloud of values of uncertain parameters or if the completed drug-related version of it should be used inside an optimization loop that would compute the best drug administration strategy.

VI. DISCUSSION

Regarding the above comparison, it is worth to mention that the knowledge-based model used in the comparison and in the data production involves some probabilistic branch that makes tight fitting of the data irrelevant. Only the global qualitative behavior and some quantitative aspect should be expected. Once this is said, one should keep in mind that the relatively low number of parameters and the easiness with which these parameters can be identified is a positive if one seeks adaptive and on-line correction of the model parameters from patient to patient or even in time for the same patient. The potential loss of representativity can therefore be highly compensated by the simplicity of the proposed model.

Regarding the way drug effect can be modeled, the following comments can be given:

- The chemotherapy can be accommodate for in a standard way using additive term (see for instance [6] and the references therein). This is because the very nature of the tumor growth proposed here are not very different from the commonly used models.
- regarding the anti-angiogenesis drugs, things are quite different. Indeed, the way the tumor induced angiogenesis is modeled here enables non standard modeling of the drug effect. Typically, according to equation (19) this drug can affect the parameters λ_r, γ_r and τ that condition the speed of the recruitment (through λ_r and τ) and the intensity of the vascular migration (through γ_r). Therefore modeling the drug u effect can be obtained by defining and identifying appropriate functions $\lambda_r(u)$, $\gamma_r(u)$ and $\tau(u)$ for which appropriate data need to be available for identification. This is an undergoing work that will hopefully be communicated later.

VII. Conclusion

In this work, a reduced model has been proposed for the drug-free tumor growth in presence of tumor induced angiogenesis. The model captures the impact of the 2D disposition of the vascular network around the tumor. It involves six easily identifiable parameters. The model enables fast simulation of the phenomena (A month can be simulated in less than 100 ms) so that extensive robustness check simulation can be easily conducted. The structure of the model offers nice opportunities to model the drug effect which is the natural follow-up of the current work.

References

[1] M. Alamir. Robust feedback design for combined therapy of cancer. *Optimal control, Applications and Methods*, 35(1):77–88, 2014.

[2] S. Chareyron and M. Alamir. Mixed immunotherapy and chemotherapy of tumors: Feedback design and model updating schemes. *Journal of Theoretical Biology*, 45:444–454, 2009.

[3] L. G. DePillis, W. Gu, and A. E. Radunskaya. Mixed immunotherapy and chemotherapy of tumor: Modeling, application and biological interpretations. *Journal of Theoeretical Biology*, 38:841–862, 2005.

[4] L. G. DePillis and A. E. Radunskaya. A mathematical tumor model with immune resistance and drug therapy: An optimal control approach. *Journal of Theoretical Medicine*, 3:79–100, 2005.

[5] P. Hahnfeldt, D. Panigraphy, J. Folkman, and L. Hlatky. Tumor development under angiogenic signaling: a dynamical theory to tumor growth, treatment, response and postvascular dormancy. *Cancer Research*, 59:4770–4775, 1999.

[6] U. Ledzewicz, H. Schattler, and A. d'Onofrio. Optimal control for combination therapy in cancer. In *47th IEEE Conference on Decision and Control*, 2008.

[7] A. Matveev and A. V. Savkin. Application of optimal control theory to analysis of cancer chemotherapy regimens. *Systems and Control Letters*, 46:311–321, 2002.

[8] M. Pons-Salort, B. Vander Sanden, A. Juhem, A. Popov, and A. Stéphanou. A computational framework to assess the efficacy of the cytotoxic molecules and vascular disrupting agents against solid tumors. *Math. Model. Nat. Phenom.*, 7(1), 2012.

[9] A. Stéphanou, S. R. McDougall, A. R. A. Anderson, and M. A. J. Chaplain. Mathematical modelling of flow in 2d and 3d vascular networks: applications to anti-angiogenic and chemotherapeutic drug strategies. *Mathematical and Computer Modelling*, 41:1137–1156, 2005.

[10] A. Stéphanou, S. R. McDougall, A. R. A. Anderson, and M. A. J. Chaplain. Mathematical modelling of the influence of blood rheological properties upon adaptative tumor-induced angiogenesis. *Mathematical and Computer Modelling*, 44:96–123, 2006.

[11] G. W. Swan. General applications of optimal control in cancer chemotherapy. *IMA Journal of mathematics Applied in Medicine & Biology*, 5:303–316, 1988.